International Journal of Plastics Technology (December 2018) 22(2):386–405
https://doi.org/10.1007/s12588-018-9211-1

RESEARCH ARTICLE

Development of value-added composites from recycled high-density polyethylene, jute fiber and flyash cenospheres: Mechanical, dynamic mechanical and thermal properties

Sukanya Satapathy[1]

Received: 31 May 2017 / Accepted: 3 October 2018 / Published online: 16 October 2018
© Central Institute of Plastics Engineering & Technology 2018

Abstract

Composites were developed from post-consumer and industrial wastes: recycled high-density polyethylene (rHDPE) and jute fiber/flyash cenospheres (FACS). Variations in mechanical strength, storage modulus (E''), loss modulus (E') and damping parameter (tan δ) with the addition of fiber/FACS into rHDPE in the presence of coupling agent maleic anhydride-grafted polyethylene (MAPE) were investigated. It was observed that the tensile strength and modulus, flexural strength and modulus as well as hardness of the composites increased significantly at 20 wt% fiber/10 wt% FACS/3 wt% MAPE with respect to rHDPE. Dynamic mechanical analysis data showed an increase in the storage and loss modulus of the both fiber/FACS-reinforced composites. The tan δ spectra presented a strong influence of fiber/FACS content and coupling agent on the α' relaxation process of rHDPE. The thermal behavior of the composites was evaluated from TGA/DTG thermograms. The fiber/FACS/matrix morphology in the MAPE-treated composites was confirmed by SEM analysis of the tensile-fractured specimens. The results suggested successful development of value-added and low-cost polymeric composites from environmentally hazardous waste materials.

Keywords Recycled high-density polyethylene · Jute fiber · Flyash cenospheres · Mechanical properties

✉ Sukanya Satapathy
sukanyarr2002@yahoo.co.in

[1] Polymers and Functional Materials Division, CSIR-Indian Institute of Chemical Technology, Hyderabad, Telangana 500007, India

Introduction

Natural fiber/thermoplastic composites find a wide array of applications in the building and construction industry such as door and window frames, decking material, railings for the parapet wall systems, furniture sections (park benches, garden chairs, etc.) and others. The most commonly used thermoplastic resins are polyethylene (PE), polypropylene (PP), polyvinyl chloride (PVC) or polyethylene terephthalate (PET). These plastics constitute the major proportion of the municipal waste stream in India and worldwide [1]. Their reuse in the production of fiber-reinforced composites is beneficial in preventing environmental pollution and cost reduction. The widely used natural fibers as reinforcements in these thermoplastic matrices include sisal, banana, hemp, coir, jute, abaca, bagasse. These natural fibers have been considered in the development of composite materials because of their superior advantages such as low density, high specific strength and modulus, renewability, biodegradability and unlimited availability [2].

Natural fiber-reinforced recycled high-density polyethylene (rHDPE) offers superior composite materials to be useful for various constructive purposes. Lei et al. [3] suggested that maleated PE (MAPE), carboxylated polyethylene (CAPE) and titanium-derived mixture (TDM) improve the compatibility between the bagasse fiber and rHDPE. The modulus and impact strength of the composites have maxima with MAPE content increase. Cui et al. [4] obtained improvement in the mechanical properties of wood fiber/post-consumer HDPE composites by the addition of coupling agent (maleic anhydride-grafted PP-MAPP). Yao et al. [5] described that rice straw fiber/virgin and rHDPE composites have comparable mechanical properties with those of wood composites. Favaro et al. [6] observed improved flexural and impact properties from the composites prepared with modified sisal fibers and unmodified post-consumer HDPE matrix. Oza et al. [7] observed that chemical treatment of hemp fibers improved the flexural strength of hemp fiber/rHDPE composites. Samariha et al. [8] found that thickness swelling and water absorption increase with the increase in bagasse fiber content in rHDPE. Aht-Ong et al. [9] suggested that PE-graft-maleic anhydride (PE-g-MA) compatibilizer can improve the properties of the composites prepared from cellulose fiber (cotton waste fabric) and recycled PE. All these studies also highlight the importance of a coupling agent/compatibilizer like MAPE or MAPP in the fiber/recycled PE system in the enhancement of the mechanical properties.

In this work, jute fiber (JF) and flyash cenospheres (FACS) were chosen as fillers for the rHDPE matrix in the presence of MAPE. JF is chosen as it is one of the cheapest natural fibers with golden and silky shine. It is the second most important vegetable fiber after cotton, in terms of usage, global consumption, production and availability. It is composed primarily of the plant materials cellulose and lignin. It falls into the bast fiber category (fiber collected from bast or skin of the plant). It is 100% biodegradable and recyclable and thus environmentally friendly. Some extensive study on this JF reinforced into different thermoplastic matrices has been done by various researchers. Wang et al. [10] studied the mechanical properties of alkali-, alkali/methyl methacrylate (MMA)- and alkali/

polyamide (APT)-treated JF-PP composites and observed a good increase in the tensile strength, flexural strength and flexural modulus in case of APT composites with better interfacial compatibility. Zaman et al. [11] studied the composites fabricated from irradiated JF-irradiated PP and irradiated coir fiber-irradiated PP at different doses (250–1000 krad). They revealed that the jute-based composites had better mechanical properties and fiber/matrix adhesion as compared to coir-based ones.

Goriparthi et al. [12] developed and studied the mechanical, thermal, viscoelastic and biodegradability properties of biocomposites based on surface-modified JF-polylactide (PLA)/polycaprolactone (PCL) blends. They observed that surface-modified JF resulted in improved tensile strength and modulus of the PLA composites with a reduction in impact toughness. However, the addition of PCL resulted in the recovery of the impact toughness without sacrifice in stiffness and strength along with an increase in the biodegradation rate of the composites. Jahan et al. [13] studied the thermal, optical and electrical properties of JF-LDPE composites and obtained good electrical properties. Lovdal et al. [14] investigated the mechanical properties of JF/polylactic acid composites as a function of ambient temperature in the range of 5–80 °C and applied micromechanical models to back-calculate the reinforcement efficiency of the JF. Their results demonstrated that the thermal sensitivity parameters like glass transition temperature and the heat deflection temperature cannot be used as sole parameters for determining the gradual change in mechanical properties of the composites.

Khan et al. [15] studied the mechanical properties of JF-PP composites by treating the JF with potassium permanganate in acid (oxalic acid and sulfuric acid) and alkaline (KOH) media to investigate the oxidizing effect on the properties of the composites. They found out that the oxalic acid-treated JF-PP composites showed better mechanical performance. The treated composites showed improved thermal stability, less water sensibility and less degradable in soil, water and simulated weathering conditions. Mina et al. [16] studied the effect of untreated and triple-super-phosphate-treated JF-isotactic PP composites prepared by compression molding technique. Both the treated and untreated composites were irradiated by gamma rays, and both produced an increase in tensile strength, flexural strength and Young's modulus. The thermal stability of the treated composites was comparatively more than the untreated ones. Siddiquee and Helali [17] fabricated JF-PE and JF-PP composites and studied the effects of fiber length and fiber ratio on the biodegradability of the composites. They observed weight loss in the composites, suggesting that the composites are biodegradable. They also observed that the higher fiber length and fiber ratio showed the highest degradation rate.

Sayeed et al. [18] investigated the tensile and flexural properties of alkali-treated JF-PP non-woven composites. They observed a significant enhancement in the flexural and tensile moduli of composites when non-wovens consisting of preferentially and non-preferentially aligned JF were stacked in an alternate manner. Gunti et al. [19] studied exclusively the mechanical and thermal properties of alkali-treated and untreated JF–polylactic acid composites. They observed that the treated fiber composites gave better flexural strength and modulus in comparison with untreated composite and neat resin. However, the impact strength of the untreated fiber/polylactic

acid composite was higher than the treated fiber composite and neat resin. The thermal degradation of the untreated fiber composites was higher than the treated one but lower than that of the pure polylactic acid resin. Ranganathan et al. [20] studied the mechanical performance and toughness of JF-PP composite using MAPP as compatibilizer and viscose fibers as impact modifiers. They found out that the soft and tough viscose fibers improved the toughness of JF-PP composites. They also observed that 2 wt% MAPP significantly improved the overall composite properties.

FACS is small proportion of the pulverized fuel ash produced in abundance, and its disposal causes considerable environmental problems. It is therefore very much necessary to investigate this inexpensive material for possible use in various systems including polymer and fiber-/polymer-based ones. These ash particles are unique free-flowing powders, hollow in nature, have ultra-low-density, low water absorption characteristics and consist of silica, iron and alumina. An enhancement in only flexural modulus and hardness values was obtained in our own study on FACS-filled coir fiber/recycled polyethylene composite system [21]. However, a significant enhancement in mechanical and dynamic mechanical properties was observed for banana fiber/FACS-reinforced rHDPE system. The tensile and flexural strength obtained were suggested to be suitable for deck boards/guardrail systems [22]. Kulkarni et al. [23] observed a better compressive strength and lowered density along with cost with the use of FA in the E-glass fiber/epoxy system. Subham and Tiwari [24] studied the mechanical properties of FA-filled E-glass fiber/epoxy composites by varying FA concentrations and modifying the FA surface by γ-amino propyl triethoxy silane coupling agent. With surface modification of FA the tensile and impact strength showed improvement resulting in good interfacial bonding and lower damping capability.

Saxena et al. [25] obtained better physical, chemical, mechanical, weathering and fire resistance properties for FA-filled jute/sisal–polyester composites than conventional materials like wood and wood substitute. They suggested that the developed composite system can be used for a number of applications like partitioning, false ceiling, roofings, panels, floorings, wall tiles, furniture. Jena et al. [26] obtained an overall improvement in mechanical properties of cenosphere-filled bamboo/epoxy composites, and they suggested that the composite strength could be effectively tailored by varying weight fraction of filler and number of layers. Dalbehera and Acharya [27] studied the effect of cenospheres as particulate filler in jute/glass–epoxy hybrid composite system. They observed that the mechanical properties were significantly increased with the addition of filler in comparison with unfilled composite also indicating good dispersibility of cenosphere in the matrix. Thus, a thorough investigation on the detailed properties of both fiber/FACS-reinforced recycled thermoplastic polymer system would be beneficial in successful development of value-added composites utilizing these waste materials as matrix and filler.

Development of composites using rHDPE as the matrix in such fiber/filler–polymer systems can solve the environmental and economical issues caused by their disposal. An effort has been made in this study to suggest the potential utility of FACS/JF-rHDPE for various outdoor applications. Mechanical, dynamic mechanical and thermal properties of rHDPE and the composites have been evaluated. The fractured surface and interfacial adhesion morphology of the composites were also observed

using scanning electron microscopy (SEM). The impact of JF/FACS on the water absorption characteristics of rHDPE has been studied.

Experimental

Materials

rHDPE recovered from disposed waste bottles of pharmaceutical companies was provided by Sneha Plastics, Hyderabad, India, and used as the matrix material. It was found to have a MFI of 0.84 g/10 min and density of 0.950 g/cc. JF was purchased from the local market, detergent washed and cut to an approximate length of 6 mm manually. Table 1 represents their physical and chemical properties. MAPE obtained from M/s Pluss Polymers, India, under the trade name OPTIM E-156 having MFI: 4.5 g/10 min and density: 0.954 g/cc was used as coupling agent. FACS (grade: 5–150 μm) was procured from Swift Services, Secunderabad. The FACS particles as observed under SEM were spherical in shape, relatively smooth and had average particle size of 125 μm [21]. They were found to have different proportions of oxides, i.e., Al_2O_3(27–33%), SiO_2(55–65%) and Fe_2O_3(6%). JF and FACS were used as reinforcing agents.

Fabrication of composites

JF-rHDPE composites were prepared by melt mixing in an intermeshing counter-rotating JSW-twin screw extruder (PR/EX/02, Japan). The JF along with rHDPE was premixed at different weight percent of fiber loading (10–30 wt%). The compounding was carried out at a screw speed of 150 rpm and temperature range of 140, 150, 160, 170 and 180 °C from the feed to die zone, respectively. The extrudates were cooled in water at room temperature, granulated in a pelletizer (HJC D75, Korea) and dried at 105 °C for 4 h to eliminate residual humidity before injection molding. For preparation of JF/MAPE-rHDPE composites, the MAPE of variable concentrations (1, 3 and 5 wt%) was compounded with JF-rHDPE composites (20 wt% JF loading) at similar conditions mentioned above

Table 1 Physical and chemical properties of JF[4,13]

Property	Values
Density (g/cm^3)	1.3–1.5
Tensile strength (MPa)	393–773
E-modulus (GPa)	13–26
Elongation at break (%)	1.17–1.5
Moisture content (%)	12.6
Cellulose (wt%)	61–72
Lignin (wt%)	12–15
Hemicellulose (wt%)	15–20

for untreated composites. Finally, the JF/FACS/MAPE-rHDPE composites were prepared. The FACS of variable concentrations (2.5, 5, 7.5 and 10 wt%) was compounded with JF-rHDPE composites (20 wt% JF loading at 3 wt% MAPE). Subsequently, the dried granules from all the mixing stages were taken for preparation of mechanical (tensile, flexural, izod impact and hardness) test specimens, according to ASTM D standards using an automatic injection molding machine (Kloner Windsor (P) Ltd., India, PR/AIM/02) at 190 °C and injection pressure of 65 psi with clamping force of 130 TONS.

Mechanical properties

Tensile properties (tensile strength, tensile modulus and elongation at break) of the prepared composites were measured as per ASTM D638 (Standard test method for tensile properties of plastics) with gauge length of 60 mm, at a crosshead speed of 10 mm/min by using Universal Testing Machine (AGS-10 KNG, Shimadzu). Flexural properties (flexural strength and modulus) were measured as per ASTM D790 (Standard test method for flexural properties of unreinforced and reinforced plastics and electrical insulating materials) with gauge length of 60 mm, at a crosshead speed of 1.3 mm/min using the same Universal Testing Machine (AGS-10 KNG, Shimadzu). Notched izod impact strength of the composite specimens was evaluated using an Impactometer (Tinius Olsen, USA) as per ASTM D256 (Standard test method for determining the izod pendulum impact resistance of plastics) with a notch depth of 2.54 mm and notch angle of 45^0 using a 7-J hammer. The shore D hardness values of the individual composites were determined according to ASTM D2240 (Standard test method for rubber property, durometer hardness) in a Shore D Hardness Tester (RR-12). Hardness is generally used to describe resistance of material to surface indentation, scratching or marring. The measurements were taken 15 s after the durometer tip had touched the sample. Tests for determination of mechanical properties were carried out in a standard temperature of 23 °C ± 2 °C and 50% ± 2% RH. The data reported are from the average of 6 specimens for each test. Corresponding standard deviations have also been reported. The mechanical properties of the composites were statistically evaluated with a one-way analysis of variance (ANOVA) followed by a post hoc Tukey HSD at 0.01 level of significance.

Dynamic mechanical properties

Specimens of rHDPE, MAPE-treated JF-rHDPE and JF/FACS-rHDPE composites having dimensions 55 mm × 10 mm × 3 mm were subjected to dynamic mechanical test using TA Instruments, DMAQ800. The measurements were taken in the bending mode of the equipment, and corresponding viscoelastic properties were determined as a function of temperature. The temperature range used in the present investigation was varied from − 50 to + 100 °C, with a heating rate of 5 °C/min, under nitrogen flow. The samples were scanned at a fixed frequency of 1.0 Hz.

Thermogravimetric analysis

JF, rHDPE and the MAPE-treated composites were subjected to thermogravimetric analysis using TA Instruments, TGAQ500. Samples of ≤ 5 mg weight were scanned from 40 to 600 °C at a heating rate of 20 °C/min in nitrogen atmosphere. The initial, final, maximum degradation temperature and the corresponding percentage weight loss were recorded.

Differential scanning calorimetry

DSC analysis of the rHDPE and the composite samples (5–10 mg) was done using TA Instruments, DSCQ100 at a heating rate of 20 °C/min in the temperature range between 30 and 200 °C in a nitrogen environment. The cooling and second heating were then done at the same rate to evaluate the thermal transition behavior of the composites. Corresponding melting temperature, heat of fusion and crystallization temperature were recorded.

Scanning electron microscopy

The tensile fractured surfaces of the composite samples were sputtered with gold and investigated under SEM (Hitachi-S520, Japan)

Water absorption test

Water absorption test of JF-rHDPE, MAPE-treated JF-rHDPE and JF/FACS-rHDPE composites was performed as per ASTM D570 (Standard test method for water absorption of plastics). Specimens were dried at 80 °C in a vacuum oven until a constant weight was attained. Subsequently, they were immersed in water in a thermo-stated stainless steel water bath at 30 °C. Weight gain was recorded by periodic removal of the specimens from the water bath and weighing on a balance with a precision of 1 mg. The percentage gain at any time as a result of moisture absorption was determined.

Results and discussion

The mechanical, dynamic mechanical and thermal properties of JF/FACS-reinforced rHDPE composites were extensively studied in order to evaluate their efficiency as developed composite material with potential application possibilities.

Mechanical properties

Effect of fiber loading

The variation of mechanical strength as a function of fiber loading (0–30 wt%) is represented in Table 2. A significant increase ($p < 0.01$) was observed in the values

of tensile strength and modulus with the increase in fiber loading from 0 to 20 wt% for JF-rHDPE composites. The tensile strength increased by 19% [25.51 MPa (±1.59) to 30.31 MPa(±1.03)] with the increase in fiber content to 20 wt%, beyond which it decreased marginally. The tensile modulus increased by 129% [146.34 MPa(±39.76) to 334.47 (±29.46)] in comparison with the unfilled rHDPE. The increase in the tensile strength owes to the high cellulose content of JF. Cellulose chains have a high resistance in tension and play an important role in the tensile strength of natural fiber-filled polymeric composites [28, 29]. The increase in tensile modulus indicated increase in stiffness of the composites. Such increase in stiffness indicated load transfer from the matrix to the fibers through the fiber/matrix interface [30, 31]. However, in the JF-reinforced rHDPE composites the elongation at break values decreased significantly suggesting decrease in ductility [30, 32].

The flexural strength and modulus of the composite samples showed a significant increase ($p < 0.01$) with fiber loading up to 20 wt%. The flexural strength increased by 16% [25.08 MPa (±0.23) to 29.08 MPa(±0.55)] and the flexural modulus by 52% [154.03 MPa(±4.95) to 234.46 MPa(±8.84)] with 20 wt% JF loading in rHDPE matrix. This increase in flexural strength suggests increased bending properties of the samples due to increased network system by the fibers having high aspect ratio [33]. On the other hand, the increased flexural modulus is due to efficient stress transfer between the polymer and fiber resulting in increased stiffness of the composites [34]. There is decrease in tensile and flexural strength properties of the composites at higher fiber loading of 30 wt%. This decrease implies poor fiber/matrix adhesion promoting microcrack formation at the interface as well as non-uniform stress transfer due to fiber agglomeration within the matrix [29].

There was a significant increase ($p < 0.01$) in the izod impact property of the JF-rHDPE composites at 10 wt% fiber loading, followed with a significant decrease up to 30 wt% fiber loading. This decrease in the impact strength of the composites was explained by some researchers as reduction in the ability of matrix to absorb energy with increase in fiber loading, thereby reduction in the toughness [35]. The shore D hardness values of the samples increased with the increase in fiber loading and were maximum at 20 wt% JF loading. This implied that the degree of resistance of the composite to indentation measured in shore durometer is high [36]. This increase in hardness values of the fiber/matrix composites also owes to the composition of fiber having a good proportion of lignin content [29].

Effect of MAPE treatment

Literature studies [37] suggest that the maleic anhydride groups of MAPE covalently link with the hydroxyl groups of the fibers forming an ester linkage. Also, the non-polar part (PE) of MAPE becomes compatible with the PE matrix and lowers the surface energies of the fibers, thereby increasing their wettability and dispersion within the matrix. As implied from the test results reported in Table 2, all the untreated composites (at 20 wt% fiber loading) exhibited an improved tensile and flexural properties. Thus, this fiber loading in the rHDPE matrix was taken for further treatment with variation in MAPE loading and to study the detail mechanical properties.

Table 2 Mechanical properties of rHDPE, MAPE-treated JF-rHDPE and JF/FACS-rHDPE composites (values in parenthesis represent standard deviations)

Sample	Tensile strength (MPa)	Tensile modulus (MPa)	Elong. at break (%)	Flexural strength (MPa)	Flexural modulus (MPa)	Izod impact strength (kJ/m^2)	Hardness shore D
rHDPE	25.51 (1.59)	146.34 (39.76)	128.02 (41.68)	25.08 (0.43)	154.03 (4.95)	22.43 (3.09)	60
JF-rHDPE (10:90)	27.63 a* (0.44)	243.31a (23.91)	38.33a (2.9)	27.14 a (0.50)	202.10a (9.73)	24.83a (4.67)	62
JF-rHDPE (20:80)	30.31 b (1.03)	334.47b (29.46)	17.48b (2.99)	29.08 b (0.55)	234.46b (8.84)	15.23b (0.75)	68
JF-rHDPE (30:70)	29.64 b (0.35)	325.95b (7.44)	15.32bc (1.56)	28.39 ab (0.28)	214.91ab (4.98)	13.4b (1.25)	65
JF/MAPE-rHDPE (20:1:79)	32.81 c (0.33)	335.56b (3.35)	10.29c (3.72)	31.22 c (1.15)	275.28c (16.88)	8.69c (0.31)	72
JF/MAPE-rHDPE (20:3:77)	33.27 c (0.43)	381.48c (24.41)	9.53bc (3.18)	32.83 d (0.64)	314.84d (5.40)	7.16c (0.63)	76
JF/MAPE-rHDPE (20:5:75)	30.96 b (0.32)	281.74ab (30.70)	9.56bc (2.34)	30.44 c (1.29)	261.49c (10.51)	5.75c (0.35)	70
JF/FACS/MAPE-rHDPE (20:2.5:3:74.5)	33.01 c (0.28)	303.44b (8.95)	52.42d (4.33)	27.97 ab (0.70)	236.42b (12.37)	8.43c (0.68)	76
JF/FACS/MAPE-rHDPE (20:5.0:3:72)	33.15 c (0.65)	347.93bc (5.24)b	26.42b (4.08)	30.44c (0.55)	287.06c (14.75)	7.05c (0.82)	78
JF/FACS/MAPE-rHDPE (20:7.5:3:69.5)	33.30c (0.87)	307.22b (30.81)	22.81b (1.0)	30.24bc (0.15)	274.47c (5.80)	7.49c (0.63)	78
JF/FACS/MAPE-rHDPE (20:10:3:67)	34.56d (0.31)	418.65c (13.60)	11.05c (0.67)	33.58d (0.19)	372.02e (20.65)	6.00c (0.50)	80

*Average values followed by different letters in the same column are statistically different at $p < 0.01$

The composites prepared at 3 wt% MAPE concentration showed a significant enhancement ($p < 0.01$) in tensile strength (9%), tensile modulus (17%), flexural strength (13%), flexural modulus (34%) and hardness (27%), respectively, with respect to the untreated composite at 20 wt% fiber loading. This phenomenon is due to increase in interfacial adhesion between the fibers and the matrix with the addition of MAPE. Lei et al. [3] have also reported similar behavior for wood and bagasse fiber-reinforced rHDPE composites upon MAPE treatment. Further increase in the MAPE concentration from 3 to 5% resulted in a significant decrease in the tensile and flexural properties. This behavior may be attributed to the self-entanglement among the MAPE chains rather than the polymer matrix resulting in slippage [21, 38].

Effect of FACS loading

The JF/MAPE-rHDPE composite samples at 20 wt% JF loading and 3 wt% MAPE showed optimum mechanical properties. This composition has been taken for fabrication with FACS and for further characterization studies. The mechanical properties of JF/MAPE-rHDPE composites containing different weight percentage of FACS (2.5, 5, 7.5 and 10 wt%) are depicted in Table 2. It was observed that with the addition of FACS particles, there was significantly no much difference in the tensile strength values of the composites from 2.5 to 7.5 wt% loading. However, there was a significant increase ($p < 0.01$) in the tensile strength with an increase in FACS content to 10 wt%. Such increase in the value of tensile strength was due to the effective dispersion of FACS in the JF/MAPE-rHDPE matrix [39]. The tensile modulus values decreased with the FACS loading from 2.5 to 7.5 wt% followed with an increase at 10 wt%. There was a significant increase ($p < 0.01$) in the values of elongation at break with the addition of FACS at 2.5, 5 and 7.5 wt%, followed with a decrease at 10 wt%. This decrease in the value of elongation at break with filler loading at 10 wt% owes to the rigid FACS particles [40] which reduced the flexibility of the polymer/fiber matrix.

The flexural strength and modulus of the JF/MAPE-rHDPE composites with variation in FACS loading from 2.5 to 10 wt% were measured. The flexural strength and modulus of JF/MAPE-rHDPE composites at 0 wt% FACS loading were found to be 32.83 MPa (± 0.64) and 314.84 MPa (± 5.40), respectively. FACS incorporation significantly decreased the flexural strength and modulus with increase in loading from 2.5 to 7.5 wt%. However, there was an increase in the flexural strength at 10 wt% FACS loading suggesting some possible mechanical anchorage between the filler/fiber and polymer matrix [41]. Also, a significant increase ($p < 0.01$) in flexural modulus value was observed at this loading indicating an enhancement in rigidity of the composites. This increase in modulus value with the addition of reinforcing filler (at 10 wt% loading) owes to effective stress transfer from the matrix to the filler at the interface [42, 43]. The notched izod impact strength of the JF/MAPE-rHDPE composites did not show any appreciable change with the incorporation of FACS from 2.5 to 10 wt% loading, owing to the stiffening of the polymer chains. Such phenomenon was also observed by Nourbakhsh and Ashori [33] in case of bagasse fiber/nanoclay–PP composites. The reduced values of impact strength in comparison

with neat matrix are due to failure mode becoming brittle, and relatively less energy is absorbed by the composite having sound dispersoid/matrix bonding allowing less energy absorption [44].

The shore D hardness values of the JF/MAPE-rHDPE composites increase with the increase in FACS loading and were maximum at 10 wt%. Similar increase in hardness values with both filler and fibers as reinforcements was obtained by Patel and Manocha [45] in case of carbon-FA/PANOX fiber composites. Further increase in FACS loading from 10 to 15 wt% showed a decrease in the mechanical properties of the JF/MAPE-rHDPE composites, and the data for the same have not been reported in this context. The mechanical findings were in agreement with the morphological interpretations from SEM as discussed in the later section. At 10 wt% FACS loading, the JF/MAPE-rHDPE composite had an increase in tensile strength and modulus, flexural strength and modulus and hardness values, suggesting that FACS acted as a reinforcing filler in the development of composites. Saxena et al. [25] suggested such developed composite materials as a potential wood substitute material. Our results corroborated with the results of Jena et al. [26], Dalbehera and Acharya [27] where they also obtained improved mechanical properties for FACS-filled JF/polyester, bamboo fiber–epoxy and JF-glass fiber hybrid/epoxy composites, respectively.

Dynamic mechanical properties

The dynamic mechanical analysis of rHDPE, MAPE-treated JF-rHDPE and JF/FACS-rHDPE composite samples was carried out to investigate the properties of the composites under dynamic loading conditions with an increase in temperature. The variation of the storage modulus (E') as a function of temperature is shown in Fig. 1a. The E' of the composites increased from that of rHDPE, with JF/FACS/MAPE-rHDPE showing the highest value. The storage modulus of rHDPE, JF/MAPE-rHDPE and JF/FACS/MAPE-rHDPE was 3132, 4178 and 5078 MPa, respectively. Thus, from the increase in the E' values, it could be inferred that an improvement in interfacial bonding [46] occurred in MAPE-treated JF-rHDPE and JF/FACS-rHDPE composites, particularly in case of both JF/FACS-filled composite, and this fully corroborates with the flexural test observations.

The variation of loss modulus (E'') as a function of temperature is shown in Fig. 1b. The E'' of MAPE-treated JF and both JF/FACS-filled composites increased with respect to rHDPE, with the highest being that for JF/FACS/MAPE-rHDPE composite. The α' transition temperature measured from the single prominent peak of the E''curves was 57, 59 and 61 °C for rHDPE, JF/MAPE-rHDPE and JF/FACS/MAPE-rHDPE, respectively. This shift in the α' transition to higher temperatures in the composites is attributed to the restriction in the mobility of the polymer chains in the crystalline phase so that more energy is required for the transition to occur [47]. The E''values at the α' transition temperature for rHDPE were 164 MPa, which increased to 273 and 299 MPa, for JF/MAPE-rHDPE and JF/FACS/MAPE-rHDPE composites, respectively.

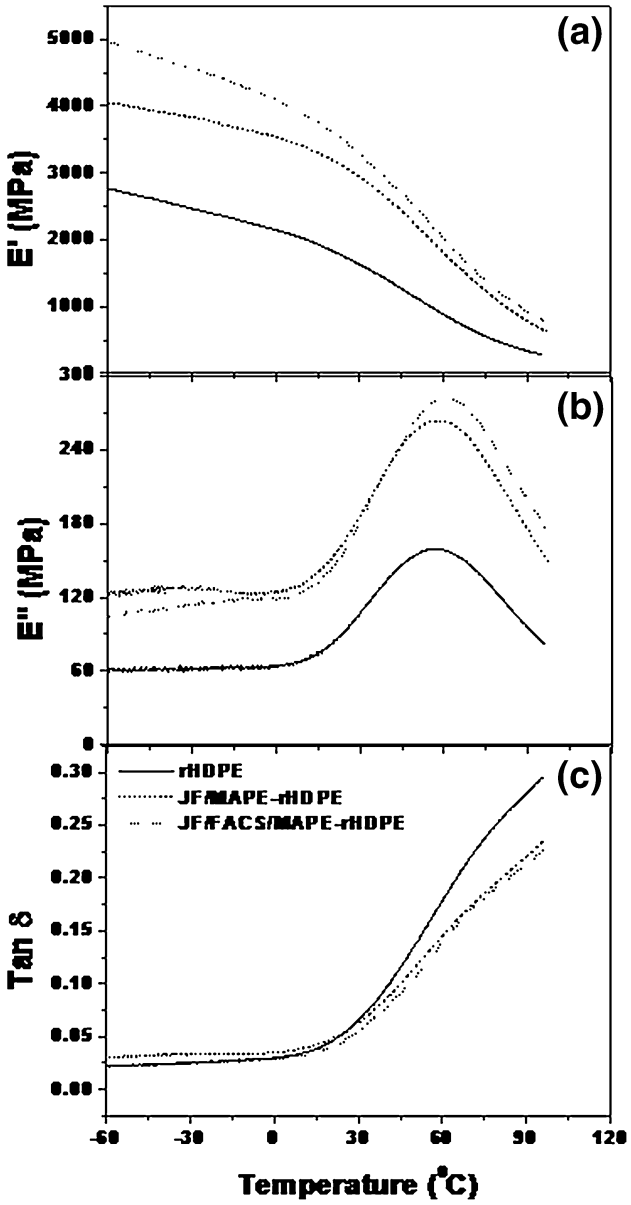

Fig. 1 Variation of **a** storage modulus, **b** loss modulus and **c** tan δ of rHDPE and the composite samples

The variation of the damping parameter (tan δ) as a function of temperature is shown in Fig. 1c. The rHDPE and its composites with JF and JF/FACS showed the same damping values, and the curves overlaid below the α' transition temperature. Above this point, the JF and JF/FACS-filled rHDPE composites showed reduction

in the damping values with respect to rHDPE. The damping values of rHDPE, JF/MAPE-rHDPE and JF/FACS/MAPE-rHDPE at the transition temperature were 0.18, 0.15 and 0.15, respectively. This decrease in damping values with addition of fiber and fiber/filler to the neat matrix indicated less energy dissipation with a stronger interface [38, 48].

Thermal properties

Thermogravimetric analysis

The TGA and DTG curves of rHDPE, JF, MAPE-treated JF-rHDPE and JF/FACS-rHDPE composites are represented in Fig. 2a, b, and the corresponding data are listed in Table 3. The onset of degradation of rHDPE began at about 461 °C, and the maximum decomposition temperature (T_{max}) appeared at about 484 °C. This decomposition range of rHDPE was comparatively higher than that of JF. In case of JF, dehydration and degradation of lignin occurred around 231–311 °C and maximum percentage of cellulose was found to decompose at a temperature of 365 °C [37, 48]. Because of the carbonization of JF, the residual weight was 19%. In the MAPE-treated JF-rHDPE and JF/FACS-rHDPE composites there were two degradation stages. One degradation stage was for the fiber added, and the other was for the rHDPE. The T_{max} for the first stage appeared at 321–390 °C for the treated JF-rHDPE and 332–395 °C for the treated JF/FACS-rHDPE composite systems, respectively. This is due to dehydration from the cellulose unit and thermal cleavage and scission of C–O and C–C bonds [37]. The T_{max} of the composites for the second stage appeared at nearly the same level as the neat rHDPE. The coupling agent seemed to have little influence on the thermal degradation of the composites. The observations were in line with that reported in the literature for MAPE-treated other natural fiber-filled rHDPE composite [3]. For the JF-rHDPE and JF/FACS-rHDPE composites, the percent residue at 600 °C is found to be higher than that obtained for neat rHDPE matrix (Table 3). This increase in percent residue in the composites with fiber/filler addition indicated higher thermal stability and improved flame-retardant properties as suggested by Saw et al. [49] in case of jute/bagasse–epoxy novolac composites.

Differential scanning calorimetry

The DSC curves of rHDPE and its composites with JF and JF/FACS are given in Fig. 3a, b. The melt crystallization temperature (T_c), crystallization enthalpy (ΔH_c) obtained from cooling cycle, and the melting temperature (T_m) and melting enthalpy (ΔH_m) values obtained from the second heating cycle are given in Table 4. The rHDPE matrix showed slightly higher melting peak (134.33 °C) with higher enthalpy values compared to its composites with fiber/filler. The lowering in T_m value for JF-rHDPE (133.67 °C) and JF/FACS-rHDPE (133.21 °C) composites in the presence of MAPE indicated that the crystallization process occurred more rapidly and those crystals formed are smaller, which is due to the nucleation effect

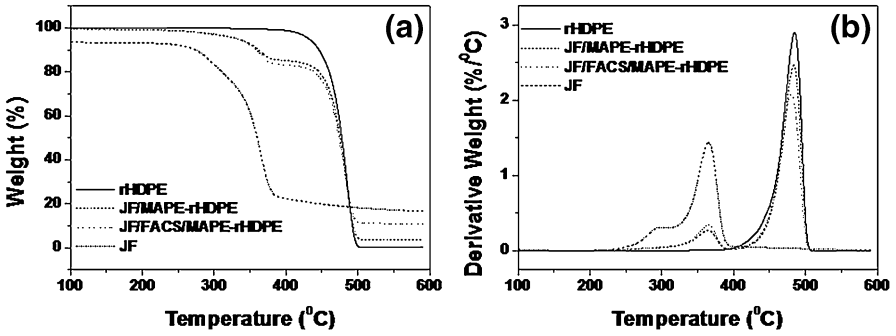

Fig. 2 **a** TGA and **b** DTG plot of rHDPE, JF/MAPE-rHDPE, JF/FACS/MAPE-rHDPE and JF

imparted by the coupling agent for the PE matrix. Thus, incorporation of fiber/filler leads to changes in the crystalline morphology of the composites influencing their thermal and mechanical properties [50]. However, the T_c values increased in JF-rHDPE (116.84 °C) and JF/FACS-rHDPE (117.21 °C) from that of rHDPE (116.25 °C), exhibiting the ease of crystallization in the presence of MAPE coupling agent [51].

The addition of JF and both JF/FACS into the rHDPE matrix in the presence of MAPE significantly reduced the melting (ΔH_m) enthalpy, crystallization (ΔH_c) enthalpy and percent crystallinity (X_c) of the polymer matrix, shown in Table 4, which is attributed to the reduction in structural regularity and close packing ability of the polymer chains in the presence of fiber/filler [51, 52]. It was observed that the X_c of rHDPE was 53.58%, which decreased to 43.58% for JF-rHDPE and 40.69% for JF/FACS-rHDPE composites. Similar lowering in crystallinity level was reported in case of bagasse fiber/rHDPE composite system [38] in the presence of MAPE coupling agent. The authors corroborated that reduction in crystallinity leads to improvement in compatibility between the phases in the composite system. The degree of crystallinity has been estimated using the following equation

$$X_c(\%) = \Delta H_m \times 100/\Delta H_{100\%}\left(1 - W_W\right)$$

where X_c is the percentage of crystallinity, ΔH_m is the experimental melting heat of fusion, $\Delta H_{100\,\%}$ is the heat of fusion of 100% crystalline HDPE (293 J/g) [3], and W_W is the weight fraction of FACS.

Scanning electron microscopy

The tensile fractured surface of JF-rHDPE, JF/MAPE-rHDPE and JF/FACS/MAPE-rHDPE composites is presented in Fig. 4a–c. Without MAPE, there was separation between the rHDPE and the fibers, as shown in Fig. 4a, because of the incompatibility between the hydrophobic matrix and hydrophilic fibers. For MAPE-treated JF-rHDPE composite, as observed from Fig. 4b, there is absolutely no fibers pull out and the fracture surface shows intimate mixing of the fibers with the polymer matrix.

Table 3 TGA data of rHDPE, JF, MAPE-treated JF-rHDPE and JF/FACS-rHDPE composites

Sample	Stage	Temperature range (°C)	T_{max} (°C)	Residue (%)
rHDPE	First	461–494	484	0.1
JF/MAPE-rHDPE	First	321–390	365	5.8
	Second	421–511	483	
JF/FACS/MAPE-rHDPE	First	332–395	365	13.3
	Second	426–514	481	
JF	First	231–311	292	19.0
	Second	323–396	365	

The fiber surfaces are fully covered with the matrix material, and no fiber surface is visible devoid of any matrix. This owes to the addition of MAPE that improved the compatibility between the fiber and matrix, in turn increasing the tensile properties significantly. From Fig. 4c, the fractured surfaces of JF/FACS/MAPE-rHDPE composite exhibited no fiber pull out and the FACS particles occupied the gaps in between the fiber and matrix resulting in improved mechanical properties of these composites as studied in our earlier section.

Water absorption test

The influence of JF and FACS on the moisture stability of JF-rHDPE and JF/FACS-rHDPE composites in the presence of MAPE is shown in Fig. 5. It is evident from the test results that there is a linear increase in the water absorption in all the samples. JF-rHDPE composite samples exhibited a greater tendency of water absorption, which is due to hydrophilic nature of JF. MAPE coupling agent in JF-rHDPE system acted as dispersing agent between the fiber and matrix [33, 53] in turn decreasing the rate of water absorption. In the case of JF/FACS-rHDPE composites, the FACS embedded within the JF-rHDPE matrix as observed from SEM analysis, created longer diffusion paths, thereby resulting in less water absorption in comparison with fiber-filled rHDPE composite systems.

Conclusion

The JF/FACS-filled rHDPE composites were evaluated for their mechanical, dynamic mechanical and thermal properties. The addition of both fiber/FACS into rHDPE matrix resulted in a significant enhancement in tensile and flexural properties. In DMA analysis, the highest increase in storage modulus and loss modulus was found in JF/FACS-rHDPE composite, with a shift in α′ transition temperature to higher value. An increase in thermal stability and flame-retardant properties of

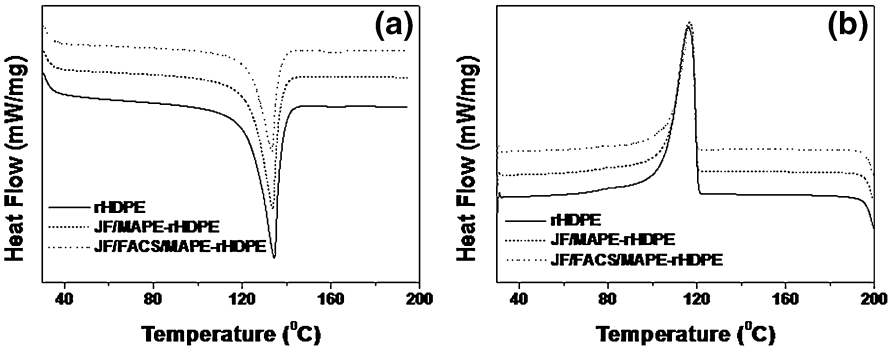

Fig. 3 DSC plots of the **a** second heating and **b** cooling cycle of rHDPE, JF/MAPE-rHDPE, JF/FACS/MAPE-rHDPE

Table 4 T_c, T_m, enthalpies (ΔH) and Xc of the rHDPE and its composites with JF as well as JF/FACS during DSC cooling and second heating cycles

Sample	DSC cooling cycle		DSC second heating cycle		X_c (%)
	T_c (^{0}C)	ΔH_c (J/g)	T_m (^{0}C)	ΔH_m (J/g)	
rHDPE	116.25	162.8	134.33	157.0	53.58
JF/MAPE-rHDPE	116.84	127.8	133.67	127.7	43.58
JF/FACS/MAPE-rHDPE	117.24	115.3	133.21	107.3	40.69

the composites was evidenced from TGA. DSC analysis also revealed that incorporation of FACS influenced the crystalline characteristics in the composites leading to changes in their thermal properties. A compatibilized interface was visible in MAPE-treated JF/FACS-rHDPE composites from the SEM analysis. This study suggests that both fiber/FACS as reinforcing agents in recycled polymeric matrix has tremendous potential and such developed composites can be used for deckings and furniture applications.

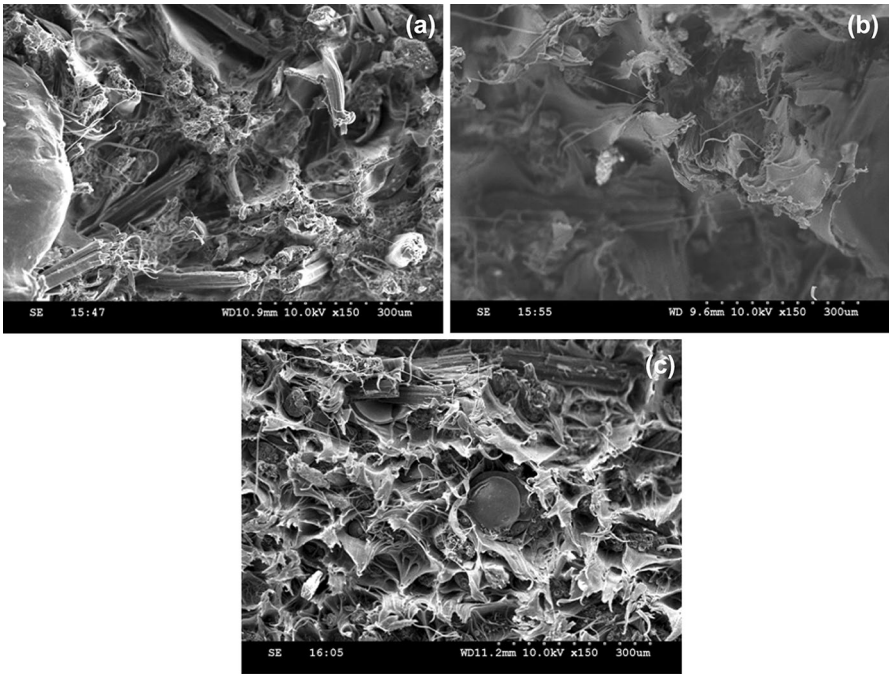

Fig. 4 SEM micrograph of **a** JF-rHDPE, MAPE-treated **b** JF-rHDPE and **c** JF/FACS-rHDPE composite samples

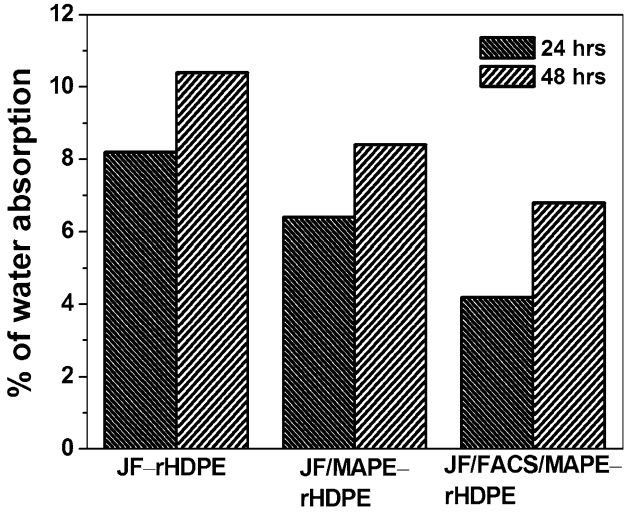

Fig. 5 Water absorption characteristics of Column 1. JF-rHDPE, Column 2. JF/MAPE-rHDPE, Column 3. JF/FACS/MAPE-rHDPE

Acknowledgements Dr. Sukanya Satapathy thanks Department of Science and Technology (DST) for financial grant under Women Scientists Scheme-A (WOS-A), Grant No. SR/WOS-A/CS-36/2016 (G). Author greatly acknowledges Central Institute of Plastics Engineering and Technology, Hyderabad, India, for the processing and izod impact testing facility for the composite samples. Author also greatly acknowledges Dr K V S N Raju and Dr. T Shekharam of Polymers and Functional Materials Division for their constant support and encouragement.

References

1. Satapathy S, Chattopadhyay S, Chakrabarty KK, Nag A, Tiwari KN, Tikku VK, Nando GB (2006) Studies on the effect of electron beam irradiation on waste polyethylene and its blends with virgin polyethylene. J Appl Polym Sci 101:715–726
2. Mitra BC (2014) Environment friendly composite materials: biocomposites and green composites. Defence Sci J 64:244–261
3. Lei Y, Wu Q, Yao F, Xu Y (2007) Preparation and properties of recycled HDPE/natural fiber composites. Compos Part A Appl Sci Manufact 38:1664–1674
4. Cui Y, Lee S, Noruziaan B, Cheung M, Tao J (2008) Fabrication and interfacial modification of wood/recycled plastic composite materials. Compos Part A Appl Sci Manufact 39A:655–661
5. Yao F, Wu Q, Lei Y, Xu Y (2008) Rice straw fiber reinforced high density polyethylene composite: effect of fiber type and loading. Indus Crops Product 28:63–72
6. Favaro SL, Ganzerli TA, De Carvalho Neto AGV, Da silva ORRF, Radovanovic E (2010) Chemical, morphological and mechanical analysis of sisal fiber-reinforced recycled high density polyethylene composites. eXPRESS Polym Lett 4:465–473
7. Oza S, Wang R, Lu N (2011) Thermal and mechanical properties of recycled high density polyethylene/hemp fiber composites. IJAST 1:31–36
8. Samariha A, Hemmasi AH, Ghasemi I, Bazyar B (2011) Short-term water absorption and thickness swelling behavior of recycled polyethylene reinforced with bagasse flour. MEJSR 8:971–974
9. Aht-Ong D, Atong D, Pechven C (2011) Surface and mechanical properties of cellulose micro fiber reinforced recycle polyethylene film. Mat Sci Forum 695:469–472
10. Wang X, Cui Y, Zhang H, Xie B (2012) Effects of methyl methacrylate grafting and polyamide coating on the behavior and mechanical properties of jute fiber reinforced polypropylene composites. J Vinyl Addit Technol 18:113–119
11. Zaman HU, Khan MA, Khan RA (2012) Comparative experimental measurements of jute fiber/polypropylene and coir fiber/polypropylene composites as ionizing radiation. Polym Compos 33:1077–1084
12. Goriparthi BK, Suman KNS, Nalluri MR (2012) Processing and characterization of jute fiber reinforced hybrid biocomposites based on polylactide/polycaprolactone blends. Polym Compos 33:237–244
13. Jahan A, Rahman MD, Kabir H, Kabir MA, Ahmed F, Hossain MA, Gafur MA (2013) Optical, electrical and thermal properties of jute and glass fiber reinforced LDPE composites. IJBAS 1:482–490
14. Lovdal A, Laursen LL, Anderson TL, Madsen B, Mikkelsen LP (2013) Influence of temperature on mechanical properties of jute/biopolymer composites. J Appl Polym Sci 128:2038–2045
15. Khan JA, Khan MA, Islam R (2013) Mechanical, thermal and degradation properties of jute fabric-reinforced polypropylene composites: effect of potassium permanganate as oxidizing agent. Polym Compos 34:671–680
16. Mina MF, Shohrawardy MHS, Khan MA, Alam AKMM, Beg MDH (2013) Improved mechanical performance of triple super phosphate treated jute-fabric reinforced polypropylene composites irradiated by gamma rays. J Appl Polym Sci 130:470–478
17. Siddiquee KM, Helali MM (2014) Effects of fiber length and fiber ratio on the biodegradability of jute polymer composites. IJSER 2:64–69
18. Sayeed MMA, Rawal A, Onal L, Karaduman Y (2014) Mechanical properties of surface modified jute fiber/polypropylene nonwoven composites. Polym Compos 35:1044–1050

19. Gunti R, Ratna Prasad AV, Gupta AVSSKS (2016) Preparation and properties of successive alkali treated completely biodegradable short jute fiber reinforced PLA composites. Polym Compos 37:2160–2170
20. Ranganathan N, Oksman K, Nayak SK, Sain M (2015) Regenerated cellulose fibers as impact modifier in long jute fiber reinforced polypropylene composites: effect on mechanical properties, morphology and fiber breakage. J Appl Polym Sci. https://doi.org/10.1002/app.41301
21. Satapathy S, Raju VSK (2015) Influence of fly ash cenospheres on performance of coir fiber reinforced recycled high density polyethylene biocomposites. J Appl Polym Sci. https://doi.org/10.1002/app.42237
22. Satapathy S, Raju VSK (2018) Mechanical, dynamic mechanical and thermal properties of banana fiber/recycled high density polyethylene biocomposites filled with flyash cenospheres. J Polym Environ. https://doi.org/10.1007/s10924-017-0938-0
23. Kulkarni SM, Kishore (2003) Effect of filler-fiber interactions on compressive strength of fly ash and short fiber epoxy composites. J Appl Polym Sci 87:836–841
24. Subham P, Tiwari SK (2013) Effect of fly ash concentration and its surface modification on fiber reinforced epoxy composite′s mechanical properties. IJSER 4:1173–1180
25. Saxena M, Morchhale RK, Asokan P, Prasad BK (2008) Plant fiber-industrial waste reinforced polymer composites as a potential wood substitute material. J Compos Mater 42:367–384
26. Jena H, Pandit MK, Pradhan AK (2013) Effect of cenosphere on mechanical properties of bamboo-epoxy composites. J Reinf Plast Compos 32:794–801
27. Dalbehera S, Acharya SK (2016) Effect of cenosphere addition on the mechanical properties of jute-glass fiber hybrid epoxy composites. J Ind Text 46:177–188
28. Wambua P, Ivens J, Verpoest I (2003) Natural fibers: can they replace glass in fiber reinforced plastics? Compos Sci Technol 63:1259–1264
29. Ayrilmis N, Jarusombuti S, Fueangvivat V, Bauchongkol P, White RH (2011) Coir fiber reinforced polypropylene composite panel for automotive interior applications. Fibers Polym 12:919–926
30. Njoku RE, Li IO, Agbiogwu DO, Agu CV (2012) Effect of alkali treatment and fiber content variation on the tensile properties of coir fiber reinforced cashew nut shell liquid (CNSL) composite. NIJOTECH 31:107–110
31. Supri AG, Aizat AE, Yazid MIM, Masturina M (2015) Chicken feather fibers-recycled high density polyethylene composites The effect of & #x03B5;-caprolactum. J Thermoplast Compos Mater 28:327–339
32. Rozman HD, Tay GS, Kumar RN, Abubakar A, Ismail H, Ishak ZM (1999) Polypropylene hybrid composites: a preliminary study on the use of glass and coconut fiber as reinforcements in polypropylene composites. Polym-Plas Technol Eng 38:997–1011
33. Nourbaksh A, Ashori A (2009) Preparation and properties of wood plastic composites made of recycled high density polyethylene. J Compos Mater 43:877–883
34. Bhagat VK, Biswas S, Dehury J (2014) Physical, mechanical and water absorption behavior of coir/glass fiber reinforced epoxy based hybrid composites. Polym Compos 35:925–930
35. Agunsoy JO, Aigbodion VS (2013) Bagasse filled recycled polyethylene bio-composites: morphological and mechanical properties study. Result Phys 3:187–194
36. Ishidi EY, Kolawale EG, Sunmonu KO, Yakubu MK, Adamu IK, Obele CM (2011) Study of physio-mechanical properties of high density polyethylene (HDPE)-palm kernel nut shell (Elaeis Guineasis) composites. JETEAS 2:1073–1078
37. Mohanty S, Verma SK, Nayak SK (2006) Dynamic mechanical and thermal properties of MAPE treated jute/HDPE composites. Compos Sci Technol 66:538–547
38. Biswal M, Mohanty S, Nayak SK (2009) Influence of organically modified nanoclay on the performance of pineapple leaf fiber reinforced polypropylene nanocomposites. J Appl Polym Sci 114:4091–4103
39. Satapathy S, Nag A, Nando GB (2013) HDPE-Fly ash/Nano fly ash composites. J Appl Polym Sci 130:4558–4567
40. Satapathy S, Nag A, Nando GB (2012) Effect of electron beam irradiation on the mechanical, thermal and dynamic mechanical properties of fly ash and nano structured fly ash waste polyethylene hybrid composites. Polym Compos 33:109–119
41. Sengupta S, Maity P, Ray D, Mukhpadhyay A (2013) Stearic acid as coupling agent in fly ash reinforced recycled polypropylene matrix composites: structural, mechanical and thermal characterizations. J Appl Polym Sci 130:1996–2004

42. Pardo SG, Bernal C, Area A, Abad MJ, Cano J (2010) Rheological, thermal and mechanical characterization of flyash-thermoplastic composites with different coupling agents. Polym Compos 31:1722–1730
43. Sreekanth MS, Bambole VA, Mhaske ST, Mahanwar PA (2009) Effect of particle size and concentration of flyash on properties of polyester thermoplastic elastomer composites. JMMCE 8:237–248
44. Malkapuram R, Kumar V, Negi YS (2009) Recent development in natural fiber reinforced polypropylene composites. J Reinforc Plast Compos 28:1169–1189
45. Patel RV, Manocha S (2013) Studies on carbon-flyash composites with chopped PANOX fibers. J Compos 2013:1–7
46. Subham P, Tiwari SK (2012) Effect of unsilanized and silanized fly ash on damping properties of fly ash filled fiber reinforced epoxy composite. In: Proceedings of the international conference on advances in aeronautical and mechanical engineering-AME, pp 20–24
47. Behzad M, Tajvidi M, Ebrahimi G, Falk RH (2004) Dynamic mechanical analysis of compatibilizer effect on the mechanical properties of wood flour-high density polyethylene composites. IJE Trans B Appl 17:95–104
48. Ray D, Sarkar BK, Basak RK, Rana AK (2004) Thermal behaviour of vinyl ester resin matrix composites reinforced with alkali treated jute fibers. J Appl Polym Sci 94:123–129
49. Saw SK, Sarkhel G, Choudhury A (2012) A Effect of layering pattern on the physical, mechanical and thermal properties of jute/bagasse hybrid fiber-reinforced epoxy novolac composites. Polym Compos 33:1824–1831
50. Sarkhel G, Choudhury A (2008) Dynamic mechanical and thermal properties of PE-EPDM based jute fiber composites. J Appl Polym Sci 108:3442–3453
51. Sengupta S, Ray D, Mukhopadhyay A (2013) Sustainable materials: value added composites from recycled polypropylene and fly ash using a green coupling agent. ACS Sustain Chem Eng 1:574–584
52. Mattos BD, Misso AL, De Cademartori PHG, De Lima EA, Magalhaes WLE, Gatto DA (2014) Properties of polypropylene composites filled with a mixture of household waste of mate tea and wood particles. Constr Build Mater 61:60–68
53. Ghasemi I, Kord B (2009) Long term water absorption behavior of polypropylene/wood flour/organoclay hybrid nanocomposite. Iran Polym J 18:683–691